

Exploration of Structure–Property Relationships by Altering Glycol Backbone Unsaturation (Double/Triple Bonds) in Furan-Based Polyesters

Virginia Arnáiz, Lucía Pedraza, Carlos Díez-Poza, Mercedes Santiago-Calvo, Enol López,* and Asunción Barbero*

This study highlights both the challenges and opportunities associated with developing bio-based furanic polyesters. Incorporating unsaturated moieties into glycol chains effectively modulates polymer rigidity and thermal properties, though it requires careful optimization of polymerization conditions. The findings demonstrate

the viability of solution polycondensation for synthesizing high-quality FDCA-based polyesters with unsaturated glycols and pave the way for further investigations into polymer design strategies that balance flexibility, thermal stability, and environmental sustainability.

1. Introduction

Plastic pollution is one of the most pressing environmental challenges of the 21st century, with only 32% of plastics being recycled at the end of their life cycle. The remaining 68% are either incinerated, releasing large emissions of polluting gases, or landfilled, with a significant portion ending up in seas and oceans. This situation has led to a great concern for introducing circular economy principles in the plastic life cycle, especially in those used in short-lived applications like packaging, which accounts for 40% of all plastic use. Poly(ethylene terephthalate) (PET), which is a condensation polyester formed from terephthalic acid and ethylene glycol, is one of the most widely used packaging plastics due to its low cost and excellent mechanical performance. However, like most plastics, PET is derived from fossil

resources and is nondegradable, contributing to the alarming problem of “white pollution.” This has driven the search for more sustainable alternatives, focusing on materials with higher recyclability and less polluting chemical additives. In response, the development of bio-based plastics from renewable raw materials has gained increasing attention from researchers and industries. One promising option is 2,5-furandicarboxylic acid (FDCA), a greener substitute for terephthalic acid in the production of polyesters. When combined with ethylene glycol, FDCA forms poly(ethylene 2,5-furanoate) (PEF),^[1–4] which is a material with PET-like properties but with a smaller environmental footprint.^[5–9] This makes PEF a strong candidate for sustainable packaging, helping to reduce reliance on fossil-based plastics and mitigate plastic pollution.^[10,11] In addition to PEF, other FDCA-based aliphatic homopolyesters have also been explored.^[1,12–15] Several works have focused on the synthesis of these furanic biopolymers, examining their thermal, structural, and, in some cases, mechanical properties.^[16–18] Among these polyesters, poly(butylene 2,5-furanoate) (PBF) has attracted special attention due to its similar properties to the homologous plastic poly(butylene terephthalate).^[19] Various studies have reported the synthesis of PBF by direct melt polycondensation of FDCA and 1,4-butanediol (BG), using tetraalkyl titanates as catalysts. An interesting study by Gross explored various reaction parameters to optimize the synthesis of poly(butylene furanoate) (PBF), reporting an optimized PBF with M_n of 23.214 g mol^{−1}.^[20] Other strategies have employed melt polytransesterification of dimethyl 2,5-furanoate and BG, again using titanium alkoxides as catalysts.^[21] Additionally, a recent approach has employed solution polycondensation of FDCA and BG in γ -valerolactone as solvent, with EDC as dehydrating agent and DMAP as catalyst.^[22] Despite its promising properties, PBF exhibits a relatively low T_g compared to other aromatic polyesters and it is nonbiodegradable. Moreover, it has a slow crystallization rate and a moderate melting temperature (T_m), which limits its broader application. Various strategies have been reported to address these limitations, including

V. Arnáiz, L. Pedraza, C. Díez-Poza, A. Barbero

Department of Organic Chemistry

Faculty of Science

University of Valladolid (UVa)

Campus Miguel Delibes, 47011 Valladolid, Spain

E-mail: asuncion.barbero@uva.es

M. Santiago-Calvo

Division of transport and energy

Fundation for Transport and Energy Research and Development (CIDAUT)

Parque Tecnológico de Boecillo, 47151 Valladolid, Spain

E. López

Department of Organic Chemistry, School of Engineering (EII)

University of Valladolid (UVa)

47002 Valladolid, Spain

E-mail: enol.lopez@uva.es



Supporting information for this article is available on the WWW under <https://doi.org/10.1002/ejoc.202500576>



© 2025 The Author(s). European Journal of Organic Chemistry published by Wiley-VCH GmbH. This is an open access article under the terms of the Creative Commons Attribution-NonCommercial-NoDerivs License, which permits use and distribution in any medium, provided the original work is properly cited, the use is non-commercial and no modifications or adaptations are made.

evaluation on the effect of glycol chain length on the properties of FDCA-derived aliphatic polyesters.^[13,23] These studies have revealed a general trend: increasing the glycol chain length tends to decrease the thermal properties, such as T_g and T_m , further highlighting the trade-off between polymer flexibility and thermal properties.

However, to our knowledge, no research has specifically investigated the impact of glycol rigidity, such as the incorporation of double or triple carbon–carbon bonds on the glycol chain. These double and triple bonds can not only affect the properties of the polymers but also enhance their degradability. Regarding chemical degradation, there are modern methods available that specifically tackle alkenes, like manganese-catalyzed photomediated oxidation with atmospheric O₂.^[24] Regarding biodegradability, the specific change from a butanediol unit to a butenediol unit was demonstrated to enhance biodegradability in polyurethanes.^[25] Therefore, we hypothesized that unsaturation can offer possibilities in both enhancing the thermal/mechanical properties and degradation ability of bioderived polyesters. Finally, a study examining the influence of various polymerization strategies (including melt polytransesterification and solution polycondensation) and reaction parameters on both the outcome of the process and the properties of the resulting biopolymers has not been reported.

In this work, we describe a detailed survey on the effect of reaction conditions (such as diol equivalents, catalyst temperature, or solvent), on both the polymerization process and the properties of various sugar-based polyesters. For that purpose, we will focus on the synthesis of furan-derived homopolymers using four-carbon chain glycols sourced from renewable materials. We will first examine the synthesis of poly(butylene 2,5-furanoate) (PBF), derived from FDCA dimethyl ester and 1,4-butylene glycol, to understand how these conditions influence polymer structure and properties. Building on these findings, we will next examine how the rigidity of the glycol chain, modified by introducing double or triple carbon–carbon bonds, affects the physicochemical properties of the final polyester.

2. Results and Discussion

2.1. Influence of Reaction Parameters in the Synthesis of Poly(butylene 2,5-Furanoate)

We began our study by systematically examining the effect of key reaction parameters—including catalyst loading, monomer stoichiometry, temperature, and reaction time—on the synthesis of poly(butylene 2,5-furanoate) (PBF) using the already known two-stage melt polytransesterification process.^[1,20,23] The first transesterification stage is typically performed between 150 and 200 °C, and the second stage, where polymerization occurs, is usually performed between 200 and 230 °C. We selected 165 °C for the first stage, as it was shown to be effective for PBF synthesis.^[1] Regarding the second stage, we fixed 215 °C, as PBF is known to undergo competitive reactions leading to bond cleavage (hydrolysis, pyrolysis) above 220 °C.^[20] In the first stage, conducted at 165 °C, transesterification of the monomers occurred, while the

second stage, carried out at 215 °C under reduced pressure, promoted the polycondensation step, leading to the formation of the final bio-based polymer. The influence of these variables on polymer conversion and polymer characteristics is summarized in Table 1.

Melt polytransesterification reactions were carried out in a three-necked round-bottomed flask suited with a refluxing-distillation system and connected to a vacuum system. The reactants (furan-2,5-dimethylcarboxylate (FDMC), 1,4-butylene glycol (BG), and Ti(O*i*Pr)₄ as catalyst) were mixed under a continuous nitrogen flow, evaluating the effect of different molar ratios of the monomers, various temperatures and reaction times, and either magnetic or mechanical stirring. As shown, under magnetic stirring, the duration of the first heating stage (165 °C) significantly influenced monomer (FDMC) conversion. Specifically, for heating times below 10 h, conversion was never complete, while full conversion was achieved (Table 1, entries 2 and 3) when the reaction was run at 165 °C between 10 and 16 h. However, small quantities of unreacted FDMC reappeared in the crude reaction with prolonged reaction time (Table 1, entry 4). As for the second heating stage (215 °C), no significant variation was observed between 2 and 4 h heating times (Table 1, entries 3 and 5). Therefore, 16 h was selected as the optimal reaction time for the first stage and 2 h for the second. In all these reactions (Table 1, entries 1–5), the BG/FDMC ratio was fixed at 2.5, resulting in the formation of polybutylene 2,5-furanoate along with varying amounts of dibutylene glycol units (DBGU) (Figure 1). Since these DBG units, formed as byproducts through the acid-catalyzed etherification of 1,4-butylene glycol,^[26] can influence the biopolymer's properties, we explored alternative reaction conditions to minimize their formation. Starting with the Ti(O*i*Pr)₄ catalyst loading, no appreciable impact on either conversion or DBGU content was observed for different catalyst loadings (2.5 vs. 5 mol%) under similar reaction conditions (Table 1, entries 3 and 6). Therefore, 2.5 mol% was selected as the optimal catalyst loading. Regarding the monomer ratio (BG:FDMC), we found that ratios below 2.5 led to unreacted FDMC (Table 1, entry 7), while an increase of this ratio to 2.7 proved beneficial, resulting in full conversion and a significant reduction in DBG units (Table 1, entry 8 vs. 3). So, we determined that under magnetic stirring, the optimal conditions correspond to entry 8.

Building on the optimal conditions established for magnetic stirring (Table 1, entry 8), we transitioned to mechanical stirring, which further improved the reaction's efficiency and scalability. Under these conditions, full conversion with no detectable DBGU content was achieved (Table 1, entry 9). We then optimized the process further by reducing the first-stage heating time to 7 h, maintaining full conversion and exclusive formation of PBF (Table 1, entry 10). A subsequent reduction to 5 h resulted in a slight decrease in conversion (93%), though DBGU formation remained absent (Table 1, entry 11). To assess the robustness of the optimized protocol, we scaled up the reaction to 5 and 20 g of FDMC under the conditions of entry 10. Both reactions proceeded efficiently (70% yield), reaching full conversion with minimal DBGU content, thereby confirming the process's scalability and reliability (Table 1, entries 12 and 13).

Table 1. Influence of reaction parameters in the synthesis of poly(butylene 2,5-furanoate) (PBF).

| Entry | Furan:glycol molar ratio | Reaction conditions | Methodology/stirring | Conversion ^{b)} | BGU:DBGU ratio ^{c)} | FDCA | RO-C(=O)-C ₄ H ₇ O-C(=O)-OR | BG | Butylene glycol units (BGU) | Dibutylene glycol units (DBGU) |
|-------|--------------------------|---------------------------|------------------------------------|--------------------------|------------------------------|------|---|-------|-----------------------------|--------------------------------|
| | | | | | | FDMC | R = Me | R = H | Conditions | |
| 1 | 1:2.5 | 165 °C/7 h 215 °C/2 h | Melt ^{a)} /magnetic | 73% | 79:21 | | | | | |
| 2 | 1:2.5 | 165 °C/10 h 215 °C/2 h | Melt/magnetic | 100% | 78:22 | | | | | |
| 3 | 1:2.5 | 165 °C/16 h 215 °C/2 h | Melt/magnetic | 100% | 79:21 | | | | | |
| 4 | 1:2.5 | 165 °C/24 h 215 °C/2 h | Melt/magnetic | 95% | 76:24 | | | | | |
| 5 | 1:2.5 | 165 °C/16 h 215 °C/4 h | Melt/magnetic | 100% | 76:24 | | | | | |
| 6 | 1:2.5 ^{d)} | 165 °C/16 h 215 °C/2 h | Melt/magnetic | 100% | 76:24 | | | | | |
| 7 | 1:1.8 | 165 °C/24 h 215 °C/2 h | Melt/magnetic | 75% | 80:20 | | | | | |
| 8 | 1:2.7 | 165 °C/16 h 215 °C/2 h | Melt/magnetic | 100% | 92:8 | | | | | |
| 9 | 1:2.5 | 165 °C/16 h 215 °C/2 h | Melt/mechanical | 100% | 100:0 | | | | | |
| 10 | 1:2.5 | 165 °C/7 h 215 °C/2 h | Melt/mechanical | 100% | 100:0 | | | | | |
| 11 | 1:2.5 | 165 °C/5 h 215 °C/2 h | Melt/mechanical | 93% | 100:0 | | | | | |
| 12 | 1:2.5 ^{e)} | 165 °C/10 h 215 °C/2 h | Melt/mechanical | 100% | 95:5 | | | | | |
| 13 | 1:2.5 ^{f)} | 165 °C/10 h 215 °C/2 h | Melt/mechanical | 100% | 90:10 | | | | | |
| 14 | 1:1 | 0 °C/2 h 15 °C/48 h | Solution ^{g)} /mechanical | 100% | 80:20 | | | | | |

^{a)}Unless otherwise specified, the melt polytransesterification reactions were conducted by mixing 2 g of FDMC with BG and 2.5 mol% of titanium isopropoxide $Ti(O^{\prime}Pr)_4$ as the catalyst; ^{b)}Conversion was calculated by integration of the PBF and FDMC signals in the 1H NMR spectrum of untreated crude samples; ^{c)}BGU:DBGU ratio was calculated by integration of the corresponding signals in the 1H NMR spectrum; ^{d)}5 mol% of $Ti(O^{\prime}Pr)_4$ was employed; ^{e)}5 g of FDMC was employed; ^{f)}20 g of FDMC was employed; ^{g)}The solution polycondensation reaction was conducted by mixing 2 g of FDCA with BG, DMAP, and EDC in 30 mL of γ -butyrolactone.

With a robust melt polytransesterification route established, we then explored an alternative synthetic pathway by preparing PBF via solution polycondensation (Table 1, entry 14). This would allow us to directly compare the structural and physical properties of polymers obtained through different methodologies, offering valuable insight into how synthesis conditions influence final material performance. For this approach, we selected 1-ethyl-3-(3-dimethylaminopropyl)carbodiimide (EDC) as dehydrating agent, 4-dimethylaminopyridine (DMAP) as catalyst, and γ -butyrolactone (GBL) as solvent. γ -Butyrolactone was chosen for its green characteristics—being biodegradable, renewable solvent, and highly polar, which improves solubility of reactants and enhances reaction efficiency. The reaction mixture was stirred for 2 h at 0 °C under nitrogen atmosphere, followed by 48 h at room temperature. The resulting solution was then washed three times with water to remove residual reagents.

Under these mild and sustainable conditions, full conversion was achieved in similar reaction yield (71%), although a small content of DBG units was present in the sample (Table 1, entry 14).

2.2. Synthesis of Other Bio-Based Furanoate Polymers with Four-Carbon Glycols

Two other FDCA-derived polymers were synthesized by melt polytransesterification using the optimal conditions established for PBF (Table 1, entry 10). These conditions were applied to *cis*-2-butene-1,4-diol and 2-butyne-1,4-diol as four-carbon chain diols, giving unsatisfactory results. Specifically, the transesterification polycondensation of FDMC with *cis*-2-butene-1,4-diol produced a brownish crude material. After dissolution in chloroform/TFA (6:1) and precipitation in methanol, the resulting polymer retained a light brown color (13% yield) and contained \approx 8 mol% residual FDMC.

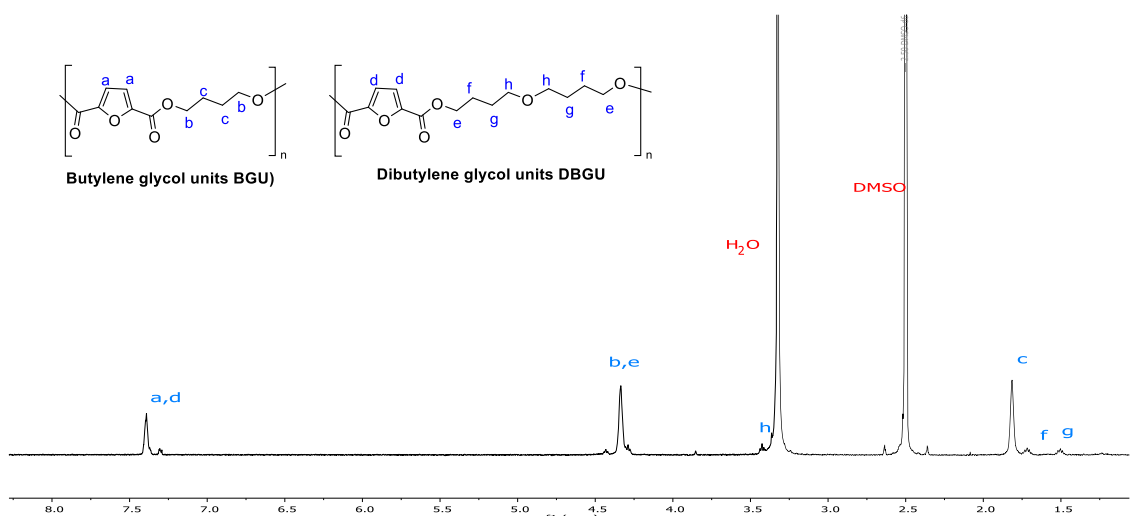


Figure 1. ^1H NMR spectrum of a PBF sample prepared by melting polytransesterification with the assignments of signals due to the DBG units.

monomer. Applying the same conditions to 2-butyne-1,4-diol resulted in the formation of a dark, tar-like product. Following two purification cycles of dissolution (chloroform:TFA, 6:1) and precipitation (methanol), a small amount of polymer was isolated (9% yield), still exhibiting a dark brown coloration and containing \approx 6 mol% FDCA monomer. These findings suggest that the elevated temperatures required for melt polycondensation likely induced partial decomposition of the diols, rendering this method unsuitable for the synthesis of these particular FDCA-based polymers (Scheme 1). This is in accordance with the literature, as different diols have been shown to need different polymerization temperatures when reacted with FDMC.

To address the issue of diol decomposition and polymer coloration under melt polycondensation, we turned to solution polymerization under milder conditions. Following the conditions stated for FDCA and BG (Table 1, entry 14), the corresponding polymerization of FDCA and *cis*-2-butene-1,4-diol afforded a white powder in good yield (67%), although ^1H NMR spectrum revealed the presence of minor impurities, indicating incomplete purification.

In contrast, the polymerization using 2-butyne-1,4-diol under the same conditions proved to be more successful. After aqueous work-up, the polymer was obtained in 78% yield as a white powder, free of residual monomer as confirmed by ^1H NMR. This

demonstrates that EDC-mediated solution polymerization in GBL is a suitable and mild alternative for synthesizing FDCA-based polyesters, particularly when the incorporation of unsaturated diols is required (Scheme 2).

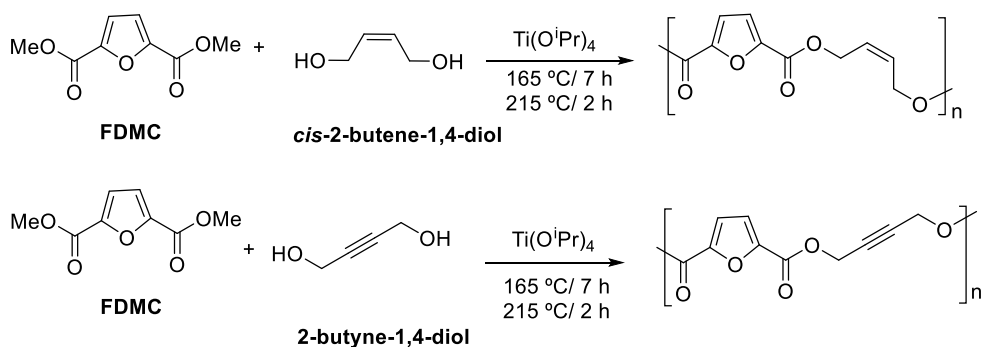
2.3. Molecular Characterization

The chemical structure of the synthesized furan-derived biopolymers was investigated using infrared spectroscopy (FTIR), as well as proton nuclear magnetic resonance spectroscopy (^1H NMR).

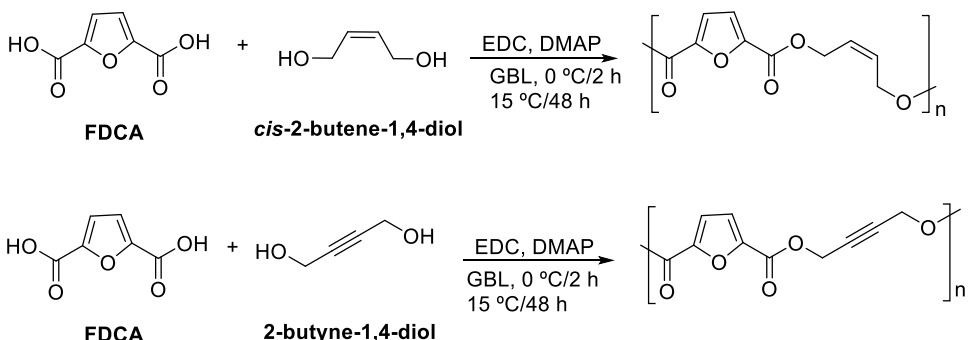
2.3.1. FTIR Analysis

The FTIR spectra of all three polymers exhibit a strong absorption band around 1719 cm^{-1} , characteristic of the ester carbonyl ($\text{C}=\text{O}$) stretching vibration. In addition, they share distinctive furanic vibrational features at 3152 , 3120 , and 1576 cm^{-1} . These bands are assigned to the asymmetric and symmetric C—H stretching modes and to the C=C vibrations of the furanyl ring.

Despite these similarities, the FTIR spectrum of poly(but-2-ene-1,4-diy furanoate) exhibits additional bands at 3029 cm^{-1} , which corresponds to C—H stretching vibrations and indicates



Scheme 1. Synthesis of other bio-based furanoate polymers with four-carbon glycols by melt polytransesterification.



Scheme 2. Synthesis of other bio-based furanoate polymers with four-carbon glycols by solution polycondensation.

the presence of vinyl moieties. In contrast, the spectrum of poly(but-2-yne-1,4-diy furanoate) lacks a distinct signal for the alkyne group. This absence can be attributed to the symmetry of the polymer's alkyne moiety, which leads to no net change in dipole moment during vibration, rendering the triple bond inactive in the infrared region (Figure 2).

2.3.2. NMR Spectroscopy

The three polymers were unambiguously characterized by NMR, with their spectra showing excellent agreement with the proposed chemical structures. Their solubility in deuterated DMSO enabled detailed ^1H analysis. In the case of poly(butylene 2,5-furanoate) (PBF), the ^1H NMR spectrum revealed the characteristic singlet of the furan ring at δ 7.2 ppm. The two distinct methylene units from the glycolic segment appeared at δ 4.5 ppm and δ 1.9 ppm, respectively. For the unsaturated poly(but-2-ene-1,4-diy furanoate), the furan proton resonances are observed at 7.42 ppm, while the vinylic hydrogens from the C–C double bond of the glycol are observed at 5.90 ppm. Additionally, the methylene group resonates at 4.98 ppm. In the ^1H NMR spectrum of poly(but-2-yne-1,4-diy furanoate), two prominent signals are detected: one at 7.51 ppm, corresponding to the furan ring hydrogens, and another at 5.10 ppm, attributed to the methylene units. These spectral features collectively confirmed the successful incorporation of the furan moieties and the expected polymer backbone structure (Figure 3–5).

2.4. Thermal Characterization

The thermal behavior of the polymer series was analyzed using differential scanning calorimetry (DSC). The DSC measurements involved a first heating, a cooling, and a second heating step to eliminate any thermal history effects. Figure 6 presents the DSC thermograms for the PBF samples obtained by different synthesis methods: the two-stage melt polytransesterification route with optimized magnetic stirring conditions (Table 1, entry 8), the same route with optimized mechanical stirring (Table 1, entry 10), and the two-stage solution polycondensation route (Table 1, entry 14).

For all three polymers, the glass transition temperature (T_g) was not detectable, likely due to their high crystallinity. As shown in

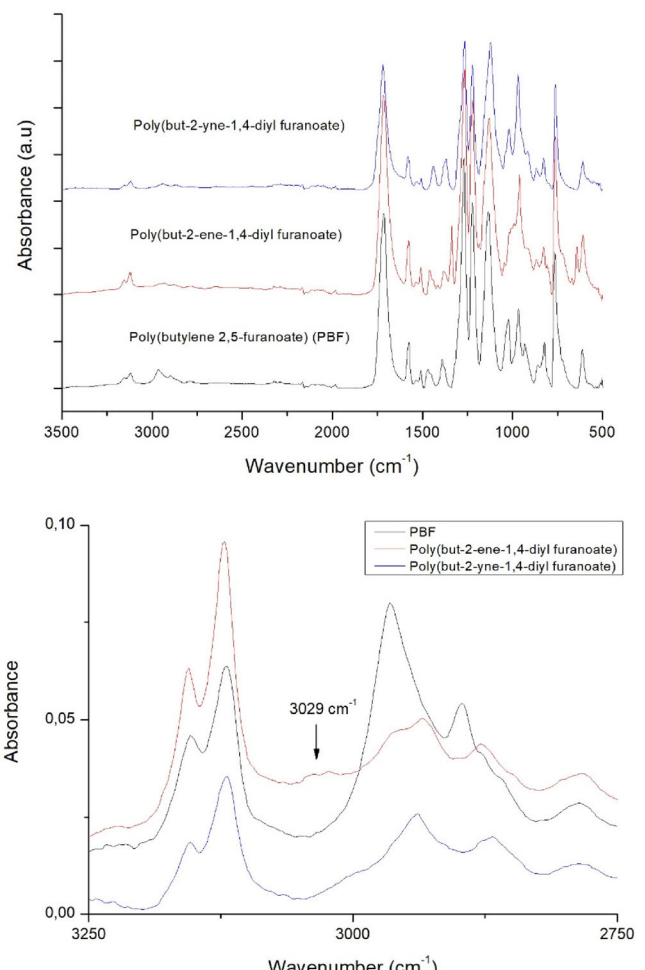


Figure 2. FTIR spectra of PBF, poly(but-2-ene-1,4-diy furanoate), and poly(but-2-yne-1,4-diy furanoate).

Figure 6, the DSC thermogram of PBF-Entry 10 exhibits a sharp cold crystallization peak (T_{cc}) at 99.4 °C, whereas PBF-Entry 14 shows a less pronounced cold crystallization peak at 87.4 °C. Additionally, the melting temperature (T_m) ranges from 168.9 °C for PBF-Entry 8 to 151.2 °C for PBF-Entry 14.

The degree of crystallinity (X_c) for the PBF samples was calculated using Equation (1), where ΔH_m is the measured melting enthalpy, ΔH_c is the cold crystallization enthalpy, and ΔH_m° is the

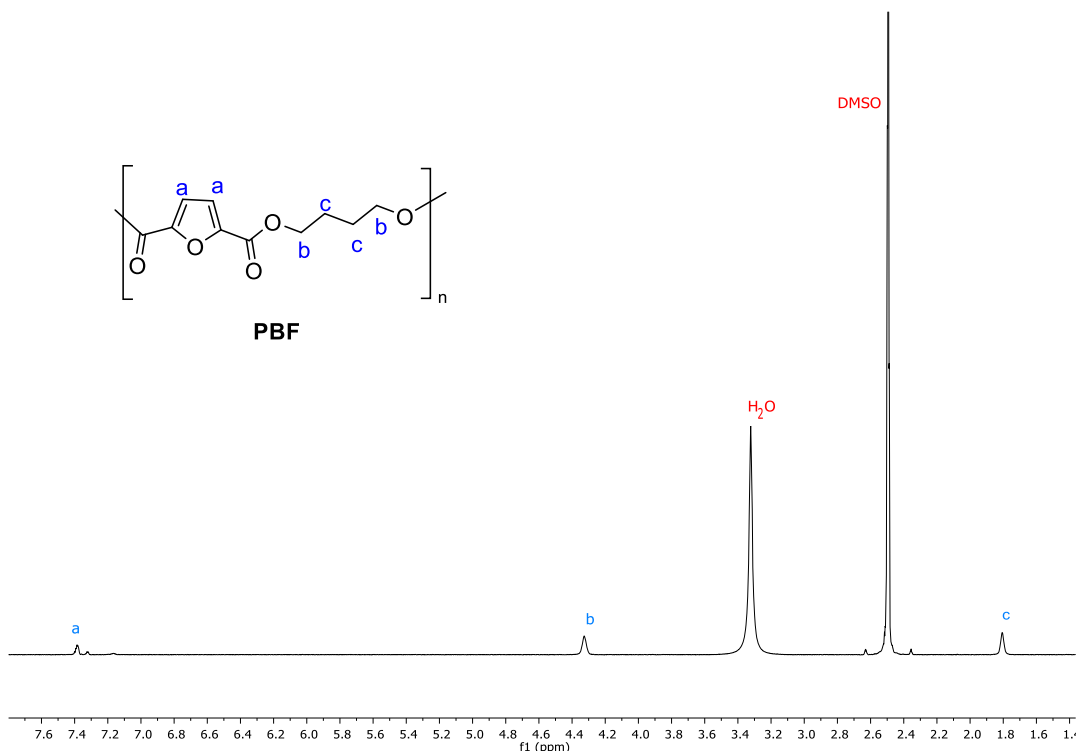


Figure 3. ¹H NMR spectrum of poly(butylene furanoate) (PBF).

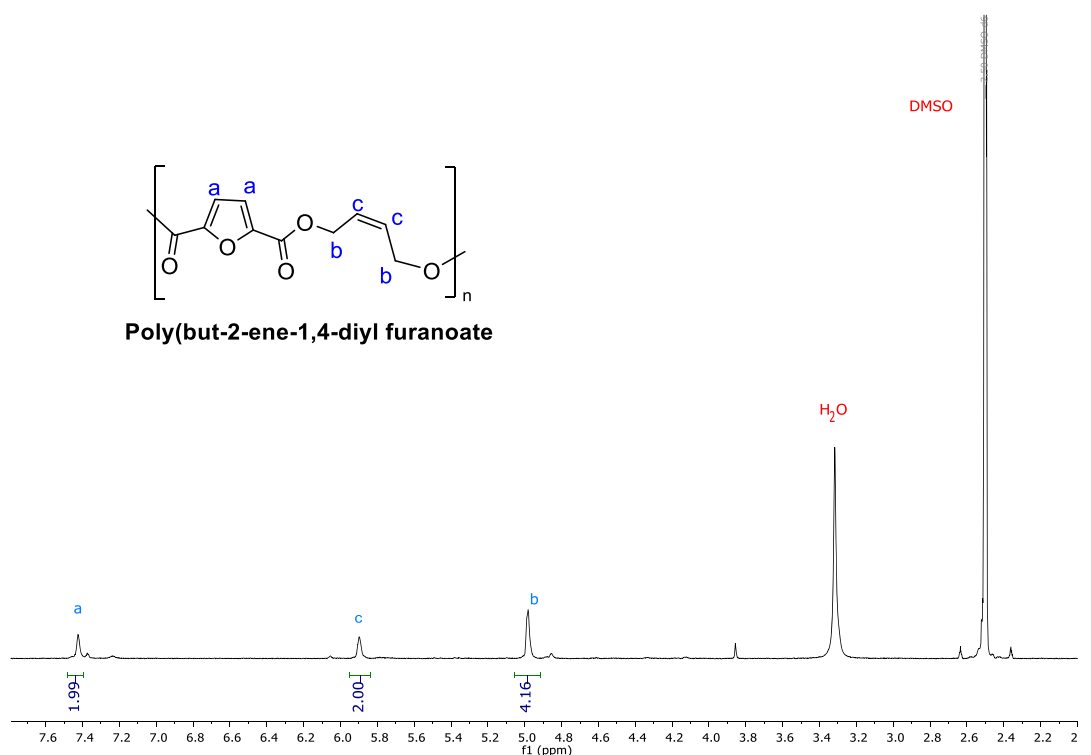
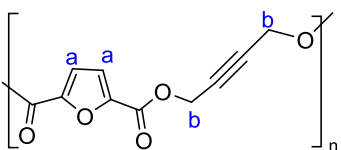


Figure 4. ¹H NMR spectrum of poly(but-2-ene-1,4-diyil furanoate).

melting enthalpy of a 100% crystalline PBF, taken as 129 J g⁻¹ from the literature.^[21] The calculated crystallinity degrees are 33% for PBF-Entry 8, 38% for PBF-Entry 10, and 43% for PBF-Entry 14.

The observed variations in crystallinity can be due to differences in their molecular weights. Generally, polymers with higher molecular weights have longer chains, resulting in reduced chain



Poly(but-2-yne-1,4-diy furanoate)

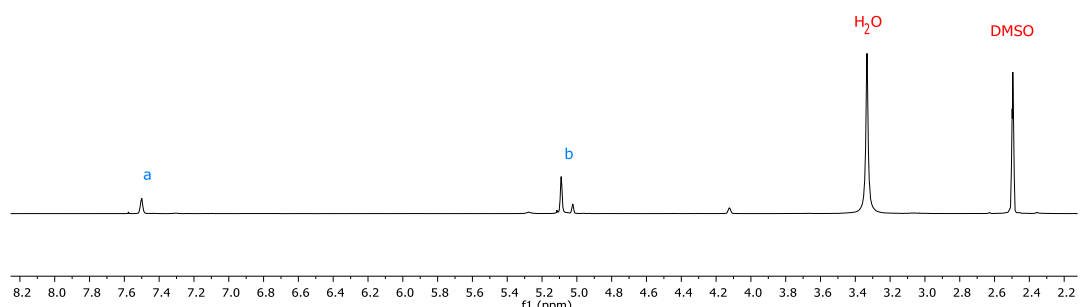


Figure 5. ^1H NMR spectrum of poly(but-2-yne-1,4-diy furanoate).

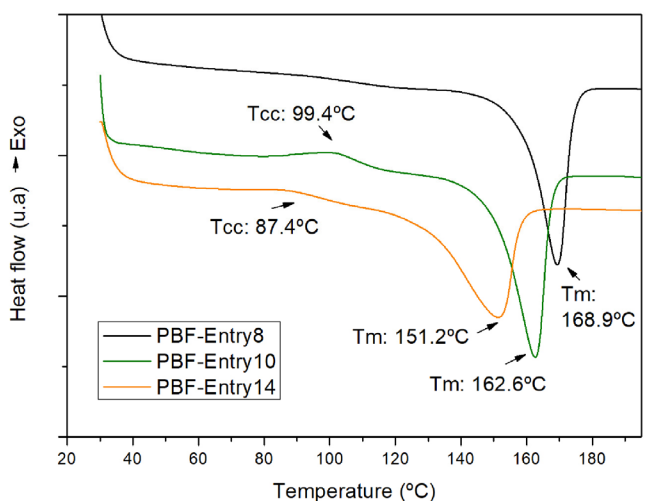


Figure 6. DSC thermogram for PBF synthesized following entries 8, 10, and 14 of Table 1.

mobility during crystallization and consequently lower degrees of crystalline order. In contrast, lower-molecular-weight polymers with shorter chains exhibit enhanced mobility, which facilitates greater molecular ordering and higher crystallinity. This effect can be seen in PBF-Entry 14 synthesized in solution that, with a lower molecular weight, demonstrates higher crystallinity (43%) compared with the melt-synthesized counterparts PBF-Entry 8 and PBF-Entry 10 (see Table 2). However, molecular weight does not fully explain the differences in the crystallization behavior

of PBF-Entry 8 (magnetic stir, melt) and PBF-Entry 10 (mechanical stir, melt). The stirring technique used throughout synthesis may also affect the molecular weight distribution.^[9] Mechanical stirring typically ensures more effective and controlled mixing compared to magnetic stirring, leading to a narrower molecular weight distribution (lower polydispersity) in PBF-Entry 10. In contrast, less controlled conditions in PBF-Entry 8 may yield broader molecular weight distributions (higher polydispersity). A more regular, narrower distribution, as expected in PBF-Entry 10, promotes more efficient packing and crystallization of the polymer chains, even at higher molecular weights. These results highlight the importance of the average molecular weight and its distribution in determining the crystallization behavior of PBF samples.

Equation (1) Degree of crystallinity

$$X_c = \frac{\Delta H}{\Delta H_m^0} = \frac{\Delta H_m - \Delta H_c}{\Delta H_m^0} \quad (1)$$

For poly(but-2-ene-1,4-diy furanoate), Figure 7 presents the DSC thermograms of the polymer synthesized via the two-stage melt polytransesterification route, optimized for mechanical stirring, and via the two-stage solution polycondensation route. It is observed that the glass transition temperature (T_g) of the polymer increases from 41.7 °C for the melt process to 51.7 °C for the solution process.

Similarly, Figure 8 shows the DSC thermograms for poly(but-2-yne-1,4-diy furanoate), produced using the same synthetic routes—melt polytransesterification and solution polycondensation.

Table 2. Intrinsic viscosity of furan-based polyesters using four-carbon glycols.

| Polymer | Methodology | Intrinsic viscosity [dL g ⁻¹] | Viscosity average molecular weight [M _v] [g mol ⁻¹] |
|------------------------------------|------------------------|---|---|
| PBF | Melt ^{a)} | 1.50 ± 0.08 | 161 183 |
| | Melt ^{b)} | 1.56 ± 0.01 | 170 080 |
| | Solution ^{c)} | 0.82 ± 0.03 | 70 475 |
| Poly(but-2-ene-1,4-diyI furanoate) | Melt ^{b)} | 1.47 ± 0.01 | 156 783 |
| | Solution ^{c)} | 0.94 ± 0.02 | 84 974 |
| Poly(but-2-yne-1,4-diyI furanoate) | Melt ^{b)} | 0.81 ± 0.02 | 69 300 |
| | Solution ^{c)} | 0.99 ± 0.02 | 91 226 |

^{a)}Melt polytransesterification under magnetic stirring (Table 1, entry 8); ^{b)}Melt polytransesterification under mechanical stirring (Table 1, entry 10 and Scheme 1);

^{c)}Solution polycondensation under mechanical stirring (Table 1, entry 14 and Scheme 2).

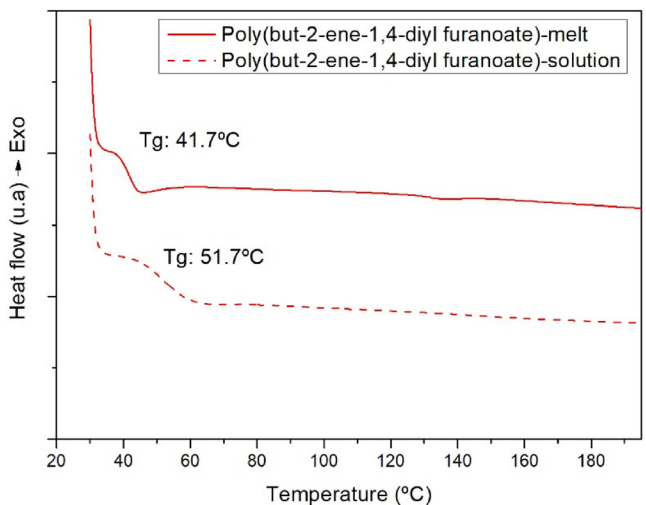


Figure 7. DSC thermogram for poly(but-2-ene-1,4-diyI furanoate) synthesized via melt and solution polycondensation.

Like poly(but-2-ene-1,4-diyI furanoate), this polymer also exhibits a higher T_g when synthesized via the solution route.

Comparing all three polymer types, the introduction of double or triple carbon–carbon bonds in the glycol chain leads to more amorphous structures. These rigid unsaturations hinder the polymer chains from aligning and packing efficiently. Furthermore, the presence of unsaturated bonds (alkene and alkyne groups) increases T_g by reducing chain flexibility. Notably, poly(but-2-yne-1,4-diyI furanoate) shows the highest T_g values for both the melt polytransesterification and solution polycondensation routes.

The thermal stability of the polymer series was analyzed using thermogravimetric analysis (TGA). Among the different synthesis routes, polymers produced via melt polytransesterification exhibited greater thermal stability compared to those synthesized through solution polycondensation. In the case of poly(but-2-ene-1,4-diyI furanoate), residual solvents from the solution synthetic protocol can cause a lower initial decomposition temperature. When comparing various polymer types, those incorporating carbon–carbon double or triple bonds degraded more rapidly than poly(butylene furanoate)s (PBF). However, these unsaturated polymers left a higher residual mass after thermal decomposition. This suggests that, despite their faster degradation onset, the presence

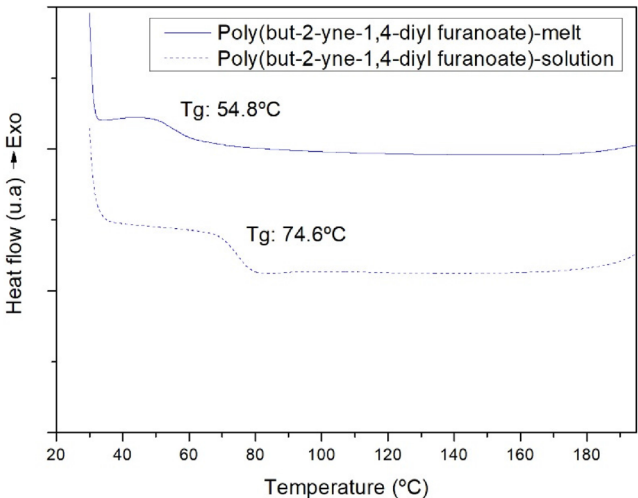


Figure 8. DSC thermogram for poly(but-2-yne-1,4-diyI furanoate) synthesized via melt and solution polycondensation.

of alkene and alkyne functional groups contributes to an improved thermal resistance at elevated temperatures (**Figure 9**). These unsaturated bonds could promote the formation of more extensively cross-linked structures which are more resistant to thermal decomposition.^[27]

2.5. Intrinsic Viscosity

Intrinsic viscosity and molecular weight are two fundamental properties of polymers, as they are closely interrelated and significantly influence the material's physical, mechanical, and thermal behavior, as well as its processability. To assess these properties, solution viscosity measurements were conducted to determine the intrinsic viscosity ($[\eta]$) of each polymer. The average viscous molecular weight (M_v) was then calculated using the Mark–Houwink–Sakurada equation (Equation (2)), where the constants K and a at 30 °C are 2.37×10^{-4} dL·g⁻¹ and 0.73, respectively, as reported for PET under similar conditions.^[28] Due to the lack of well-established parameters reported for PBF due to its novelty, we used widely accepted PET values as an approximation using ASTM D4603-00 standard protocol, which provides a

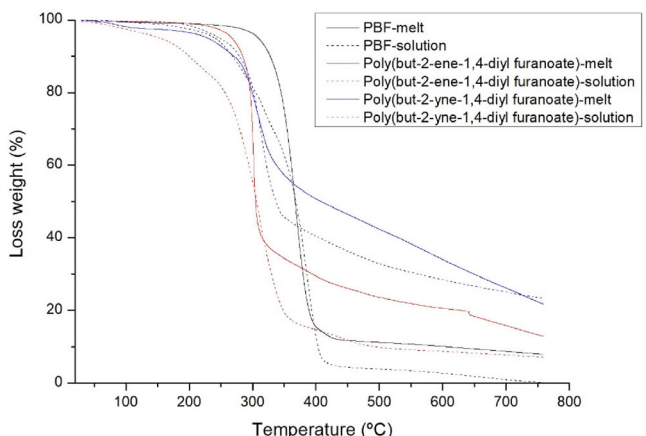


Figure 9. TGA of PBF, poly(but-2-ene-1,4-diy furanoate), and poly(but-2-yne-1,4-diy furanoate).

consistent methodology based on our experimental conditions. This strategy has been previously used in the literature.^[29]

Equation (2) Mark–Houwink–Sakurada equation

$$[\eta] = K \cdot M_v^a \quad (2)$$

Intrinsic viscosity and molecular weight are particularly useful for evaluating the effectiveness of chain extenders during PBF synthesis. Table 2 presents the $[\eta]$ and M_v values for each polymer, synthesized under the conditions listed in Table 1 (entries 8, 10, and 14).

Poly(butylene furanoate) (PBF) synthesized via melt polytransesterification using magnetic stirring (entry 8) and mechanical stirring (entry 10) exhibits comparable $[\eta]$ and M_v values. Both show higher molecular weights than the PBF synthesized by solution polycondensation (entry 14). This trend aligns with the melting temperature data shown in Figure 6, where the solution-synthesized polymer (entry 14) exhibits a lower melting point, consistent with its lower molecular weight.

For poly(but-2-ene-1,4-diy furanoate), the polymer synthesized via optimized melt polytransesterification with mechanical stirring (conditions of Table 1, entry 10) shows higher $[\eta]$ and M_v compared to its counterpart obtained via solution polycondensation (conditions of Table 1, entry 14)—a similar trend to that observed for PBF. However, poly(but-2-yne-1,4-diy furanoate) exhibits the opposite behavior: the sample synthesized via solution polycondensation demonstrates higher intrinsic viscosity and molecular weight than the one produced by the melt route. Nevertheless, since PET values were used to calculate the molecular weight of our polymers, these values should be considered approximate. More accurate molecular weight determinations will be conducted using gel permeation chromatography analysis in future studies and results will be reported in due course.

Overall, comparing the three polymer types reveals that the incorporation of unsaturated moieties (alkene and alkyne functional groups) affects the properties of the polymer following two different trends. For the melt process, a higher degree of unsaturation tends to result in lower intrinsic viscosity and molecular

weight. This is related to possible depolymerization under the applied conditions in the case of poly(but-2-ene-1,4-diy furanoate) and poly(but-2-yne-1,4-diy furanoate). Further optimization of the polymerization conditions is under investigation in our group, and results will be reported in due course. For the solution process, the higher the degree of unsaturation, the higher the intrinsic viscosity and molecular weight. Thus, the solution polycondensation methodology is a promising way of synthesizing this novel poly(but-2-yne-1,4-diy furanoate) with high molecular weights. Moreover, this confirms that structural modifications introducing unsaturations can influence chain rigidity and intermolecular interactions in FDCA-based polyesters, ultimately affecting the polymer's molecular characteristics. When comparing the melt and solution synthesis processes, significantly higher molecular weights are observed for PBF and poly(but-2-ene-1,4-diy furanoate) when synthesized via the melt method. This result is in accordance with previous studies, which also report higher molecular weights for PBF obtained through melt polymerization^[23] compared to solution polymerization.^[22] This difference can be attributed to the nature of the solution process, where lower temperatures and greater dilution necessitate longer reaction times. These factors increase the likelihood of chain termination events, leading to lower molecular weights. In contrast, the melt process employs higher temperatures and shorter reaction times, favoring the formation of polymers with higher molecular weights. However, in the case of poly(but-2-yne-1,4-diy furanoate), the very low molecular weight obtained via the melt process suggests that the reaction temperature is not optimal for this particular diol, as previously discussed.

3. Conclusion

Our study aimed to expand the potential of FDCA-derived polymers by synthesizing a series of bio-based polyesters with varied diol structures, particularly focusing on comparing saturated and unsaturated glycol chains (with alkene and alkyne groups). A systematic, comparative investigation of reaction variables and methodologies on the polymerization of PBF was conducted. Extension of the optimized conditions to unsaturated diols (*cis*-2-butene-1,4-diol and 2-butyne-1,4-diol) employing high-temperature melt polytransesterification faced challenges, such as polymer degradation and poor yields, likely due to the thermal instability of the diols. However, switching to a milder solution polycondensation method, particularly with EDC-mediated polymerization in GVL, led to significantly improved polymer quality and yields, particularly for poly(but-2-yne-1,4-diy furanoate).

Thermal analysis via DSC and TGA revealed that the incorporation of double and triple bonds increased the polymers' glass transition temperature (T_g) by reducing chain flexibility and promoting more rigid molecular structures, though it also reduced crystallinity. These modifications improved thermal resistance at elevated temperatures, despite faster degradation onset. Molecular weight and intrinsic viscosity measurements further confirmed the effects of polymerization conditions and glycol unsaturation. While melt polytransesterification generally produced higher molecular weights for saturated glycols (like in

PBF), unsaturated glycols exhibited lower molecular weights under the same conditions, likely due to side reactions or depolymerization. Conversely, solution polycondensation proved highly effective for unsaturated diols, yielding higher molecular weights and intrinsic viscosities, particularly in the case of poly(but-2-yne-1,4-diyi furanoate).

Overall, our study demonstrates that strategic variations in diol rigidity—achieved via controlled introduction of C=C and C—C bonds—provide a versatile handle to tune crystallinity, thermal transitions, degradation profiles, and molecular weight in FDCA-derived polyesters. Moreover, EDC-mediated solution polycondensation in green solvents (e.g., GBL) emerges as a particularly promising route for accessing high-performance, unsaturated biopolymers under mild conditions. These insights lay the groundwork for the rational design of next-generation, bio-based materials that balance sustainability with tailored physical properties, and they pave the way for further optimization of reaction parameters and catalyst systems to fully harness the potential of furanic polymers.

4. Experimental Section

Materials

2,5-Furandicarboxylic acid (FDCA) 97% (Cymit), 1,4-butanediol (BD), (Z)-but-2-ene-1,4-diol, but-2-yne-1,4-diol, and titanium isopropoxide (TTIP) (Sigma-Aldrich) were used as purchased.

Dimethyl Furanoate Synthesis

In a 500 mL two-neck flask, 2,5-furandicarboxylic acid (FDCA) (9.4 g, 60 mmol) was weighed and placed under N₂ atmosphere. Then, the reagent was dissolved in MeOH anhydrous (60 mL) and was added 1.6 mL of sulfuric acid (H₂SO₄) (30 mmol). The reaction mixture was heated at 75 °C for 5 h. After the reaction time had elapsed, the solvent was removed under reduced pressure. The obtained white solid was washed with a saturated NaHCO₃ solution, filtered, and left to dry in the oven for 24 h, giving the diester in 95% yield as a white solid. ¹H NMR (400 MHz, DMSO-d₆): δ 7.42 (s, 2 H), 3.85 (s, 6 H). This was a known compound and the spectroscopic data were identical to those reported in the literature.^[1]

Bulk Polymer Synthesis Using Titanium Isopropoxide [Ti(OiPr)₄]

Under a nitrogen atmosphere, FDCA dimethyl ester (2.00 g, 10.86 mmol, 1.0 equiv.) and the corresponding diol (2.5 equiv.) were introduced into a 100 mL three-necked round-bottom flask equipped with a mechanical stirrer and a reflux condenser. The mixture was heated to 115 °C for 10 min before the addition of titanium isopropoxide [Ti(OiPr)₄] (0.08 mL, 0.272 mmol, 2.5 mol%). The temperature was then increased to 165 °C and maintained for 7 h. Subsequently, the temperature was raised to 215 °C under vacuum, and the reaction continued for an additional 2 h.

After cooling to room temperature, 10 mL of a chloroform:TFA solution (6:1 v/v) was added to dissolve the crude product. The resulting

solution was poured into cold methanol and placed in a freezer overnight to promote polymer precipitation. The precipitated polymer was collected by vacuum filtration and dried in an oven.

Solution Polymer Synthesis via EDC Coupling

In a nitrogen-purged three-necked round-bottom flask, FDCA (2.00 g, 12.81 mmol, 1.0 equiv.), the corresponding diol (1.0 equiv.), and DMAP (1.56 g, 12.81 mmol, 1.0 equiv.) were combined. A solution of EDC (5.97 g, 38.44 mmol, 3.0 equiv.) in 30 mL of γ-butyrolactone was then added dropwise. The reaction mixture was stirred at 0 °C for 2 h and subsequently at room temperature for 48 h.

Following the reaction, the mixture was poured into water or methanol to precipitate the polymer. The solid was collected by vacuum filtration, washed three times with small amounts of water, and dried in an oven.

Acknowledgements

V.A. and L.P. contributed equally to this work. The authors are grateful for financial support by the Spanish Ministry of Science and Innovation and European Union Next Generation EU/PRTR TED2021-131705B-C21 and the Regional Government of Castilla y León (Junta de Castilla y León) (grant VA074G24) Complementary R+D+i Plan in the Area of Advanced Materials C17.I1 Framework of aid for Technological Centres of Excellence, Cervera CIDAUT is also grateful for RED MARFIL (CER-20231001), funded by the CDTI (Centre for the Development of Industrial Technology) through the Ministry of Science and Innovation, within the framework of aid for Technological Centres of Excellence, “Cervera.”

Conflict of Interest

The authors declare no conflict of interest.

Data Availability Statement

The data that support the findings of this study are available in the supplementary material of this article.

Keywords: biopolymers • four-carbon glycols • poly(butylene furanoate) • structure–property relationships • sugar-derived monomers

- [1] R. J. I. Knoop, W. Vogelzang, J. van Haveren, D. S. van Es, *J. Polym. Sci. Part A: Polym. Chem.* **2013**, *51*, 4191.
- [2] A. Codou, N. Guigo, J. van Berkel, E. de Jong, N. Sbirrazzuoli, *Macromol. Chem. Phys.* **2014**, *215*, 2065.
- [3] J. Wu, H. Xie, L. Wu, B. G. Li, P. Dubois, *RSC Adv.* **2016**, *6*, 101578.
- [4] G. Z. Papageorgiou, V. Tsanaktis, D. N. Bikaris, *Phys. Chem. Chem. Phys.* **2014**, *16*, 7946.
- [5] J. G. Van Berkel, N. Guigo, J. J. Kolstad, N. Sbirrazzuoli, *Macromol. Mater. Eng.* **2018**, *303*, 1700507.
- [6] V. Tsanaktis, D. G. Papageorgiou, S. Exarhopoulos, D. B. Bikaris, G. Papageorgiou, *Cryst. Growth Des.* **2015**, *15*, 5505.

[7] L. Maini, M. Gigli, M. Gazzano, N. Lotti, D. N. Bikiaris, G. Z. Papageorgiou, *Polymers* **2018**, *10*, 296.

[8] C. F. Araujo, M. M. Nolasco, P. J. A. Ribeiro-Claro, S. Rudic, A. J. D. Silvestre, P. D. Vaz, A. F. Sousa, *Macromolecules* **2018**, *51*, 3515.

[9] K. Su, W. Luo, B. Xiao, Y. Weng, C. Zhang, *Ind. Crops Prod.* **2025**, *223*, 120184.

[10] S. Weinberger, J. Canadell, F. Quartinello, B. Yeniad, A. Arias, A. Pellis, G. M. Guebitz, *Catalysts* **2017**, *7*, 318.

[11] A. Pellis, K. Haernvall, C. M. Pichler, G. Ghazaryan, R. Breinbauer, G. M. Guebitz, *J. Biotechnol.* **2016**, *235*, 47.

[12] A. Gandini, A. J. D. Silvestre, C. P. Neto, A. F. Sousa, M. Gomes, *J. Polym. Sci., Part A: Polym. Chem.* **2009**, *47*, 295.

[13] M. Jiang, Q. Liu, Q. Zhang, C. Ye, G. Zhou, *J. Polym. Sci., Part A: Polym. Chem.* **2012**, *50*, 1026.

[14] G. Z. Papageorgiou, D. G. Papageorgiou, Z. Terzopoulou, D. N. Bikiaris, *Eur. Polym. J.* **2016**, *83*, 202.

[15] V. Tsanaktsis, Z. Terzopoulou, M. Nerantzaki, G. Z. Papageorgiou, D. N. Bikiaris, *Mater. Lett.* **2016**, *178*, 64.

[16] L. Genovese, N. Lotti, V. Siracusa, A. Munari, *Materials* **2017**, *10*, 1028.

[17] G. Papamokos, T. Dimitriadis, D. N. Bikiaris, G. Z. Papageorgiou, G. Floudas, *Macromolecules* **2019**, *52*, 6533.

[18] G. Guidotti, M. Soccio, M. C. García-Gutiérrez, E. Gutiérrez-Fernández, T. A. Ezquerro, V. Siracusa, A. Munari, N. Lotti, *ACS Sustainable Chem. Eng.* **2019**, *7*, 17863.

[19] A. F. Sousa, C. Vilela, A. C. Fonseca, M. Matos, C. S. R. Freire, G.-J. M. Gruter, J. F. J. Coelho, A. J. D. Silvestre, *Polym. Chem.* **2015**, *6*, 5961.

[20] J. Zhu, J. Cai, W. Xie, P.-H. Chen, M. Gazzano, M. Scandola, R. A. Gross, *Macromolecules* **2013**, *46*, 796.

[21] G. Z. Papageorgiou, V. Tsanaktsis, D. G. Papageorgiou, S. Exarhopoulos, M. Papageorgiou, D. N. Bikiaris, *Polymer* **2014**, *55*, 3846.

[22] J. Yi, Y. Dai, Y. Li, Y. Zhao, Y. Wu, M. Jiang, G. Zhou, *ChemSusChem* **2024**, *17*, e202301681.

[23] G. Guidotti, M. Soccio, M. C. García-Gutiérrez, T. Ezquerro, V. Siracusa, E. Gutiérrez-Fernández, A. Munari, N. Lotti, *ACS Sustainable Chem. Eng.* **2020**, *8*, 9558.

[24] H. Chen, X. Guan, P. Zhang, D. Sathe, J. Wang, *Cell Rep. Phys. Sci.* **2024**, *5*, 102104.

[25] M. Burelo, I. Gaytán, H. Loza-Tavera, J. A. Cruz-Morales, D. Zárate-Saldaña, M. J. Cruz-Gómez, S. Gutiérrez, *Chemosphere* **2022**, *307*, 136136.

[26] M. B. Banella, J. Bonucci, M. Vannini, P. Marchese, C. Lorenzetti, A. Celli, *Ind. Eng. Chem. Res.* **2019**, *58*, 8955.

[27] T. P. Kainulainen, V. Gowda, J. P. Heiskanen, M. S. Hedenqvist, *Polym. Degrad. Stab.* **2022**, *200*, 109960.

[28] B. H. Bimestre, C. Saron, *Mater. Res.* **2012**, *15*, 467.

[29] N. Poulopoulou, G. Kantoutsis, D. N. Bikiaris, D. S. Achilias, M. Kapnistis, G. Z. Papageorgiou, *Polymers* **2019**, *11*, 937.

Manuscript received: June 17, 2025

Revised manuscript received: August 19, 2025

Version of record online: September 15, 2025